Available online at www.sciencedirect.com
SCIENCE DIRECT®
Journal of Magnetic Resonance 176 (2005) 87–98
JMR Journal of Magnetic Resonance
www.elsevier.com/locate/jmr

Temperature dependence of the ^{1}H chemical shift of tetramethylsilane in chloroform, methanol, and dimethylsulfoxide

Roy E. Hoffman [a], Edwin D. Becker [b,*]

[a] Department of Organic Chemistry, Institute of Chemistry, Safra Campus, The Hebrew University of Jerusalem, Givat Ram, Jerusalem 91904, Israel
[b] National Institute of Diabetes and Digestive and Kidney Diseases, National Institutes of Health, Bethesda, MD 20892-0520, USA

Received 1 March 2005; revised 17 May 2005
Available online 29 June 2005

Abstract

The chemical shift of tetramethylsilane (TMS) is usually taken to be zero. However, it does vary slightly with temperature, having obvious implications for studies of temperature effects on chemical shifts. In this work, we measure the variation in the chemical shift of TMS with temperature in three solvents, $CDCl_3$, CD_3OD, and DMSO-d_6, relative to the resonant frequency of ^{3}He gas, which can be reasonably assumed to be temperature independent. In all three solvents, the average temperature coefficient over a wide temperature range is about -6×10^{-4} ppm/°C, a factor of five smaller than that previously reported in the literature. Data are included for ^{3}He resonance frequencies over a temperature range of −110 to +180 °C, along with new measurements of volume magnetic susceptibilities of the three solvents and estimates of their temperature dependence. A novel method is used to provide temperature measurement via ^{2}H resonances of methanol and ethylene glycol samples, which can concurrently be used for field/frequency locking.
Published by Elsevier Inc.

Keywords: TMS chemical shift; ^{3}He resonance; Temperature measurement; Magnetic susceptibility; Shape factor

1. Introduction

Tetramethylsilane (TMS) is widely used as a reference for measuring proton chemical shifts and, in dilute solution, has been recommended by the International Union of Pure and Applied Chemistry (IUPAC) as a universal reference for all nuclides [1]. When data obtained at different sample temperatures are compared, the implicit assumption is often made that the chemical shift of TMS does not vary with temperature, but that assumption has no theoretical basis.

Direct measurement of frequency and magnetic field cannot be achieved to anything near an accuracy of 0.001 ppm so indirect methods are required to compare chemical shifts under varying physical conditions. The "absolute" temperature dependence of the chemical shift of TMS and several solvents used as field-frequency locks was first investigated in 1973 by Jameson and Jameson [2]. They described an experiment by Meinzer [3] to use a capillary containing a reference material placed outside the Dewar containing the sample in order to maintain a fixed reference as sample temperature varied. However, the results were found to be critically dependent on the exact location of the capillary, and the method appeared to be impractical in obtaining reliable results. As an alternative, the Jamesons reasoned that the chemical shift of a monatomic gas at low pressure should be independent of temperature, since there are no vibrational or rotational modes to excite, and the effect of collisions could be negated by extrapolation of the data to zero pressure.

In a pioneering experiment [2], they measured the resonance frequency of ^{129}Xe as a function of temperature

* Corresponding author. Fax: +1 301 435 2413.
E-mail address: tbecker@nih.gov (E.D. Becker).

1090-7807/$ - see front matter. Published by Elsevier Inc.
doi:10.1016/j.jmr.2005.05.015

and pressure (20–120 amagats—atmospheres at 0 °C at constant volume) relative to TMS and relative to several lock solvents, contained in an annular space surrounding the xenon sample. They fitted their data, extrapolated to zero pressure, over a temperature range of −33 to +27 °C, to a quadratic. They recognized that the volume magnetic susceptibility of TMS would vary with temperature, but they ignored what they felt was a small effect. This work was extended to lower pressures by Jameson et al. [4], but again the effect of magnetic susceptibility was not taken into account.

In 1982, Grant and co-workers [5] measured the magnetic susceptibility of neat TMS over the range 20 to −60 °C and used those data to correct the results of Jameson et al. [4]. They extended the work to the ^{13}C resonance of TMS. For the ^{1}H resonance, their data fitted a quadratic equation well, and they found that the TMS chemical shift moved 0.267 ppm to lower frequency as temperature increased from −60 to +20 °C. This represented an *average* temperature coefficient of -3.3×10^{-3} ppm/deg over this range.

A task group is currently conducting an IUPAC project to extend the recommendations of 2001 [1] to account for effects of solvent, temperature, magnetic susceptibility, and various solid-state effects [6]. After reviewing the previous work on temperature dependence, we concluded that a further experimental study was desirable because of several limitations in the earlier work:

- The published results refer to neat TMS, whereas the IUPAC recommendation [1] is for a solution of TMS in $CDCl_3$ at a volume fraction of 1% or less.
- The chemical shift of ^{129}Xe is known to be very sensitive to its environment [7] because of the high polarizability of the Xe atom. Moreover, Jameson et al. [4] measured ^{129}Xe at concentrations of 3–28 amagats. As ^{129}Xe has a chemical shift pressure dependence of 0.548 ppm/amagat [7], this required an extrapolation of more than 1.6 ppm from the lowest measured pressure in order to observe an effect of about 0.2 ppm over an 80 °C temperature range. Although extrapolation of the data to zero pressure should, in principle, eliminate the effects of collisions, the introduction of inaccuracies in the extrapolation would be minimized by using ^{3}He, where a low polarizability and a chemical shift sensitivity to environment 2 orders of magnitude less than xenon [8] should greatly reduce molecular interactions.
- Although the earlier studies were carried out carefully, they relied on the state-of-the-art spectrometers operating at 90 or 100 MHz for ^{1}H NMR. Current technology should lead to more precise and accurate results.
- The highest temperature was limited to the boiling point of neat TMS, whereas for TMS in $CDCl_3$ and other solvents, measurements could be made over a wider temperature range.

Accordingly, we have determined the ^{1}H chemical shift of TMS in $CDCl_3$, CD_3OD, and DMSO-d_6 relative to the ^{3}He chemical shift in helium gas over a wide temperature range. Because it was not possible to measure ^{1}H and ^{3}He spectra in a single probe, our approach was to measure the ^{3}He resonance in a coaxial sample tube with an external deuterium lock (DMSO-d_6 or the methyl resonance of CD_3OD) in one probe, then measure the ^{1}H resonance of TMS in $CDCl_3$, CD_3OD or DMSO-d_6 relative to the same lock substances in another probe. Finally, a correction was applied for the magnetic susceptibility of the TMS solution. Susceptibility effects for the lock substances cancelled in the two experiments.

As described below, we find an average temperature coefficient of about -6×10^{-4} ppm/deg for the ^{1}H chemical shift of TMS in each of the three solutions. This is a factor of five smaller than that previously reported for neat TMS [5], based on the xenon data [4].

2. Experimental

2.1. Instrumentation

NMR measurements were made on a Bruker DRX 400 spectrometer (^{1}H TMS resonance 400.13 MHz). ^{1}H NMR was measured using a 5 mm BBI probe and ^{3}He measurements were made using a similar BBI probe taken from a 300 MHz spectrometer, tuned to the helium frequency of the 400 MHz spectrometer (304.816 MHz) and the BB channel for lock [9]. ^{2}H NMR was measured using both probes. The assumed deuterium shifts for the solutions were as provided by the spectrometer manufacturer relative to a basic frequency of 61.42239123 MHz at 0 ppm. All the ^{1}H and ^{3}He spectra were acquired with deuterium lock to the methyl of methanol-d_4 at 61.42259392 MHz (basic frequency +3.30 ppm) or DMSO-d_6 at 61.42254417 MHz (basic frequency +2.49 ppm). All samples were spun at 20 Hz to reduce instability arising from convection [10,11] and allowed to equilibrate for at least 15 min before acquisition. The helium probe could not be tuned to 400 MHz proton, so temperature calibration had to be achieved with deuterium spectra of methanol-d_4 and ethylene glycol (natural abundance deuterium). ^{3}He spectra were acquired with a single pulse for the 2.2 amagat sample. A 90° ^{3}He pulse duration was achieved in 6.5 μs. The natural line-width of the resulting signal was about 1 Hz and with 1 Hz line broadening the signal-to-noise was about 90:1. For low-pressure samples, up to 256 pulses were acquired (90° pulse, 3.5 s acquisition time) to provide adequate S/N. These non-optimum pulse parameters were chosen on the basis of a preliminary inversion-recovery measurement that indicated a

very short T_1. However, the true relaxation time was later found to be quite long, approximately 1000 s, by observing the buildup of signal arising from small angle (5°) excitation as a function of the time after insertion into the magnet.

2.2. Sample tubes

Samples were measured in a 5 mm tube containing a sealed 4 mm tube attached to a 3 mm tube (Fig. 1). In some samples, the tube was closed in the middle with solid glass. The lock and temperature calibration solvent or mixture was in the outer tube while the ^{3}He gas or TMS in $CDCl_3$, DMSO-d_6 or CD_3OD was sealed in the inner tube. For high-pressure samples, the tubes were annealed and tested in an oil bath before being inserted into the spectrometer to reduce the risk of damaging the instrument.

The shape of the tubes affects the shape factor and hence the magnetic susceptibility correction by as much as 0.012 ppm. Therefore it is important to record the shape of the tube. For the inner tube, the inner diameters were 1.70 and 2.48 mm and the outer diameters were 2.94 and 4.06 mm for the lower and upper parts, respectively. The first helium sample had a concentration of 2.2 amagats and was used for whole temperature range. Another similar low-pressure helium sample was used to determine pressure dependence, which was found to be negligible. The second helium sample was closed in the middle to check for the effect on resonant frequency of convection at high temperatures, an effect that was also found to be negligible. The first $CDCl_3$ sample was used for temperatures up to 70 °C. The second $CDCl_3$ tube and the CD_3OD sample, closed at the center, were used for higher temperatures so that the liquid would not evaporate to the top of the tube. For these tubes closed at the center, the sample was introduced from the bottom, and the resultant seal added about 5 mm glass thickness, as indicated in Fig. 1. The amount of liquid was chosen to allow for expansion at high temperature without quite filling the narrow tube.

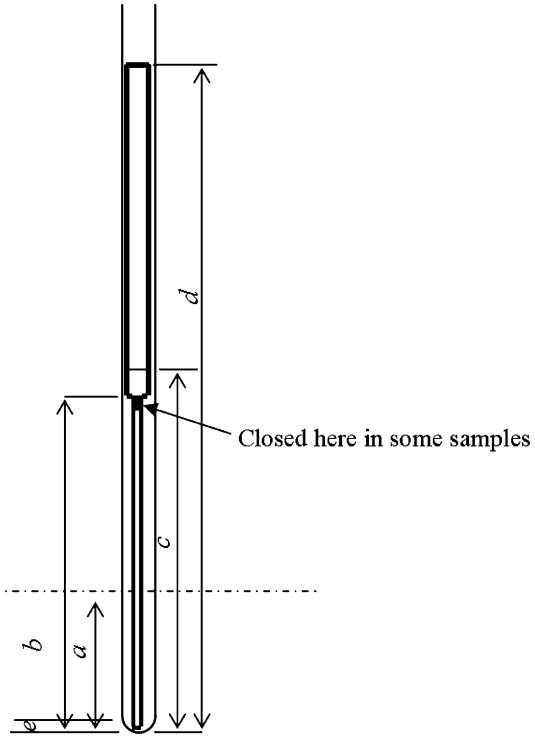

Fig. 1. Sample tube arrangement, with dimensions of inner tubes given below. See text for definitions of distances *a*–*e*.

Sample	*a* (mm)	*b* (mm)	*c* (mm)	*d* (mm)	*e* (mm)	V_0 (μL)	Closed
Helium 1	20	55	—	108	1.4		No
Helium 2	20	56	—	106	4.5		Yes
$CDCl_3$ 1	20	54	62.3	100	0.7	160.9	No
$CDCl_3$ 2	20	57	45.6	108	4.5	93.3	Yes
DMSO-d_6	20	61.5	52.4	109	1.1	116.4	No
CD_3OD	20	59.6	49.4	111	5.6	99.4	Yes

The height of the center of the receiver coil above the bottom of the outer tube is designated *a* in Fig. 1. The height of the bottom of the liquid above the bottom of the outer tube is indicated by *e*. The liquid depth (actually the height of the liquid above the bottom of the outer tube—*c* in Fig. 1) was measured at 22 °C and calculated for other temperatures using an empirical fit to the published density data for chloroform, DMSO, and methanol [12], which should provide a good approximation to the density dependence of the deuterated derivatives. Details are given in Appendix A. Expansion of the glass was considered negligible.

2.3. Sample preparation

^{3}He gas 99.9% from ICON, methanol-d_4 99.8% + atom D from Aldrich and DMSO-d_6 99.9% atom D that contained 0.4% water from Aldrich were used without further purification. Ethylene glycol was dried under vacuum at room temperature to a pressure of 0.05 mbar. Regular methanol was dried by reacting with a little potassium then distilling under vacuum. A stock solution of 3.0% v/v DMSO-d_6 in ethylene glycol was sealed in several ampoules that were opened immediately before use. $CDCl_3$ and TMS were dried with P_2O_5 and vacuum transferred. $CDCl_3$ was transferred at room temperature while TMS was transferred from a dry ice/acetone bath (−80 °C) to reduce the transfer rate. Even so, opening the TMS valve for 1 s was sufficient. The resulting 'chloroform' sample was found to contain 0.04% TMS in $CDCl_3$ 99.76% atom D. The second 'chloroform' sample that was used for high-pressure measurements contained 0.08% TMS. The DMSO-d_6 sample contained 0.2% TMS, and the methanol-d_4 sample contained 0.3% TMS.

The pressure of the ^{3}He was determined by reference to a standard sample of ^{3}He@C_{60} in 1-methylnaphthalene-d_{10}. This was chosen because ^{3}He@C_{60} is stable on a geological time-scale [13] while helium gas diffuses through glass on a time-scale of weeks [14]. The amount of helium in the standard was determined by quantitative ^{13}C NMR comparing the C_{60} signal with the solvent signal and deconvolution of the C_{60} signal into its four components, from low to high field: ^{3}He@C_{60} (142.386), C_{60} (142.362), $^{*[5,6]}C_{60}$ (142.349—with a neighboring ^{13}C across a bond between a hexagon and a pentagon) and $^{*[6,6]}C_{60}$ (142.342—with a neighboring ^{13}C across a bond between two hexagons). The standard was 0.62 mM in ^{3}He.

The gas was introduced into a Pyrex tube at about 0.7 bar (measured with a Bourdon gauge) with the tube cooled in liquid nitrogen. The tube was flame sealed and returned to room temperature. Comparison of the ^{3}He signal with the standard showed that the concentration was 2.2 amagats. A second tube was prepared with 0.1 amagats of ^{3}He with no nitrogen cooling. The concentration of the ^{3}He samples is estimated to be accurate to ±10%.

2.4. Temperature measurement method

Because the ^{3}He probe does not permit ^{1}H measurements, we determined sample temperature using the deuterium spectra of methanol-d_4 and of (natural abundance) ethylene glycol in a manner similar to that introduced (for proton NMR) by Van Geet [15,16]. For measurements of ^{3}He and of TMS, the CD_3OD or glycol was placed in the outer sample chamber (Fig. 1). At lower temperature, the CD_3 resonance of methanol-d_4 served as a lock resonance, but for higher temperatures we locked on the CD_3 resonance of dimethylsulfoxide-d_6, which was added (3.0% volume percent) to the ethylene glycol.

In separate experiments, the CD_3–OD chemical shift separation was determined as a function of temperature by comparison with the CH_3–OH separation of methanol or the CH_2–OH separation of glycol, with methanol-d_4 in the outer tube and regular methanol or glycol in the inner tube, using the temperature curves published by Amman et al. [17]. For ethylene glycol, we found no significant difference (<0.001 ppm) in the ^{1}H separation of the neat liquid compared with ethylene glycol containing 3.0% DMSO-d_6 at room temperature or at high temperature. The deuterium chemical shift separation was therefore compared with the proton separation for a single sample using the calibration of Amman et al. [17] or with a dual sample with glycol in the inner tube and regular methanol in the outer tube. While Amman only measured glycol up to 143 °C, Kaplan et al. [18] measured it up to 166 °C and found the dependence to be linear. Amman et al. claim a precision of ±0.2 °C, and Kaplan claims a precision of ±0.5 °C, but absolute accuracy is more difficult to estimate. A quadratic fit can be made to compromise between the two results while maintaining the claimed precisions at most temperatures. Eq. (1) relates the temperature (°C) to the proton chemical shift difference (ppm) in ethylene glycol:

$$T(\mathrm{CH_2OH})_2 = -0.39\left({}^{\mathrm{H}}\Delta\delta\right)^2 - 100.91\,{}^{\mathrm{H}}\Delta\delta + 192.62. \quad (1)$$

3. Results

3.1. Temperature calibration

For deuterated methanol, ^{1}H and ^{2}H spectra were obtained relative to ordinary methanol and ethylene glycol as described above. Table 1 shows the measured proton and deuterium chemical shift separations and the temperatures deduced from the calibration curve of Amman et al. [17] for methanol and from Eq. (1) for ethylene glycol. A temperature calibration curve derived for the deuterium spectrum of methanol-d_4 is shown in Fig. 2.

The same procedure was carried out for ethylene glycol in the 3.0% DMSO-d_6 in ethylene glycol sample. The temperatures shown in Table 2 are derived from Amman et al. [17] and from Eq. (1). A temperature calibra-

Table 1
Chemical shift separation of deuterated methanol compared with regular methanol and glycol

	T (°C)	$^{\mathrm{D}}\Delta\delta$ (CD_3OD)
$^{\mathrm{H}}\Delta\delta$ (CH_3OH)		
2.581	−104.1	2.588
2.518	−94.7	2.500
2.452	−85.1	2.424
2.423	−80.9	2.393
2.351	−70.8	2.319
2.277	−60.6	2.244
2.198	−50.0	2.165
2.114	−39.1	2.080
2.028	−28.1	1.992
1.941	−17.4	1.905
1.850	−6.5	1.812
1.755	4.4	1.717
1.655	15.5	1.617
1.550	26.8	1.510
1.449	37.0	1.409
1.345	47.1	1.304
$^{\mathrm{H}}\Delta\delta$ ($CH_2OH)_2$		
1.847	4.9	1.736
1.719	18.0	1.625
1.568	33.4	1.484
1.401	50.5	1.317
1.309	59.9	1.217
1.165	74.6	1.062
1.014	89.9	0.891
0.894	102.1	0.749
0.773	114.4	0.592
0.654	126.4	0.434

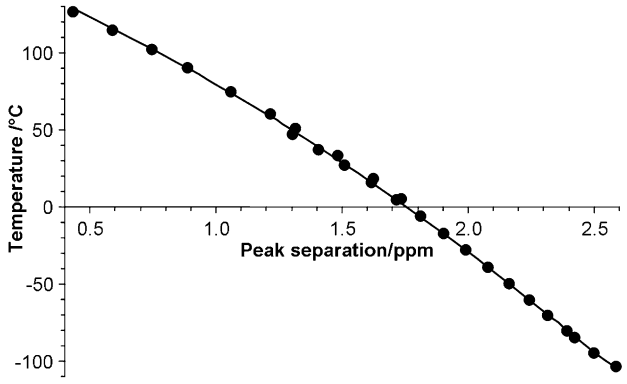

Fig. 2. Temperature calibration curve. CD_3–OD peak separation in methanol-d_4, from ^{2}H data in Table 1:

$$T_{CD_3OD} = -14.68\left(^{D}\Delta\delta\right)^2 - 65.06\,^{D}\Delta\delta + 159.48 + 3.8\times10^{-15}e^{-13.2\Delta\delta}. \quad (2)$$

For temperatures above −70 °C a quadratic fit is satisfactory. The exponential term was added to accurately model a slight deviation from a quadratic near the solvent's freezing point and is so small that it can be ignored for temperatures above −70 °C.

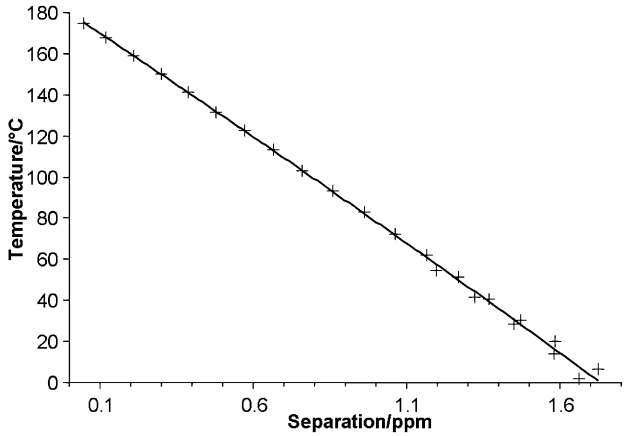

Fig. 3. Temperature calibration curve. Natural abundance deuterium peak separation of ethylene glycol in a solution of DMSO-d_6 (3.0%) in glycol, from ^{2}H data in Table 2:

$$T_{(CH_2OH)_2} = -2.80\left(^{D}\Delta\delta\right)^2 - 98.26\,^{D}\Delta\delta + 189.71. \quad (3)$$

A linear fit showed systematic deviation from the data, but a quadratic fit was about as good as a cubic fit.

Table 2
Proton and deuterium chemical shift separation for ethylene glycol

T (°C)	$^{D}\Delta\delta$ $(CH_2OH)_2$
$^{H}\Delta\delta$ (CH_3OH)	
1.778	1.8	1.762
1.671	13.8	1.682
1.532	28.6	1.549
1.402	41.7	1.423
1.266	54.6	1.298
$^{H}\Delta\delta$ $(CH_2OH)_2$		
1.831	6.5	1.824
1.701	19.8	1.684
1.601	30.1	1.571
1.497	40.7	1.468
1.394	51.2	1.369
1.287	62.1	1.267
1.186	72.4	1.163
1.082	83.0	1.061
0.981	93.2	0.961
0.883	103.2	0.859
0.785	113.2	0.764
0.692	122.6	0.671
0.602	131.7	0.580
0.508	141.3	0.488
0.421	150.0	0.400
0.332	159.0	0.308
0.245	167.8	0.220
0.175	175.0	0.147

tion curve derived for the natural abundance deuterium spectrum of ethylene glycol is shown in Fig. 3.

3.2. Helium resonance frequencies

The frequency of ^{3}He was measured for approximately each 10 °C from −110 °C (super-cooled methanol) to 185 °C (just beyond the maximum recommended temperature for the spectrometer). For temperatures below 11 °C, the ^{3}He frequency was measured relative to the deuterium resonance of the methyl of methanol-d_4 at 61.42259392 MHz. For temperatures above 63 °C, the frequency was measured relative to DMSO-d_6 (3.0%) in $(CH_2OH)_2$ at 61.42254417 MHz. Between 11 and 63 °C both references were used.

The possibility of pressure dependence for the resonance frequency of ^{3}He was examined by comparing samples at 2.2 and 0.1 amagats at 25 and 120 °C. The frequency was measured to be dependent on concentration by 0.1 ppb/amagat. This is smaller than the experimental error and was therefore ignored. Seydoux et al. [8] also reported negligible pressure dependence up to 30 atm for dissolved ^{3}He. Because the ^{3}He measurements are central to this study and are unlikely to be repeated in other laboratories, we carried out a few measurements with another sample of density 2 amagats. Data obtained agreed with the initial measurements to within 2 Hz.

^{3}He frequencies are given in Table 3 and Fig. 4. The least squares best fits of these data (frequency in Hz, temperature in °C) at low temperature (Eq. (4)) and higher temperature (Eq. (5)) are:

$$\nu\,(\mathrm{He}) - 304815000 = -0.727T + 665.51 \text{ relative to } CD_3OD, \quad (4)$$

$$\nu\,(\mathrm{He}) - 304815000 = -6.67\times10^{-4}T^2 - 0.351T + 782.07 \text{ relative to DMSO-}d_6. \quad (5)$$

These equations were used for interpolation to obtain frequencies at temperatures that correspond to those

Table 3
Observed frequency of ^{3}He

T (°C)	$\Delta\delta$ (ppm)	^{3}He frequency (MHz)	Deuterium reference
−109.7	2.644	304.8157441	$CD_3OD = 61.42259392$
−100.3	2.550	304.8157383	
−87.9	2.452	304.8157309	
−78.2	2.379	304.8157234	
−68.8	2.308	304.8157160	
−58.9	2.232	304.8157085	
−48.9	2.155	304.8157010	
−37.7	2.067	304.8156917	
−27.2	1.982	304.8156843	
−16.5	1.895	304.8156772	
−5.5	1.803	304.8156695	
5.5	1.709	304.8156611	
16.5	1.611	304.8156535	
27.9	1.509	304.8156456	
39.5	1.401	304.8156372	
51.4	1.288	304.8156286	
63.4	1.169	304.8156193	
11.2	1.734	304.8157795	DMSO-$d_6 = 61.42254417$
16.1	1.690	304.8157755	
27.3	1.587	304.8157711	
40.6	1.461	304.8157672	
52.1	1.352	304.8157626	
62.9	1.251	304.8157583	
76.4	1.121	304.8157495	
87.1	1.017	304.8157452	
97.4	0.918	304.8157404	
108.6	0.809	304.8157364	
119.1	0.707	304.8157310	
129.9	0.600	304.8157259	
139.3	0.507	304.8157205	
149.9	0.402	304.8157152	
160.3	0.297	304.8157097	
169.8	0.202	304.8157041	
179.4	0.105	304.8156980	
185.4	0.042	304.8156914	

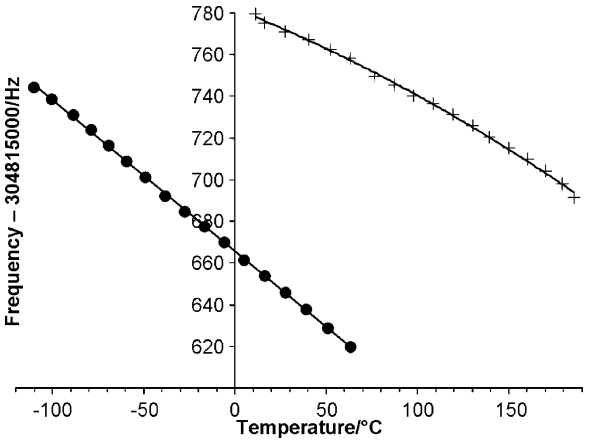

Fig. 4. Observed NMR frequency of ^{3}He relative to a deuterium lock of: (●) CD_3 resonance of methanol-d_4; (+) CD_3 resonance of DMSO-d_6 (3% solution in ethylene glycol).

used for the TMS studies described below. No physical meaning should be ascribed to the functional form.

3.3. TMS in $CDCl_3$, DMSO-d_6, and CD_3OD

The frequency of TMS in $CDCl_3$ (Table 4, column 3) was measured from −70 °C, (super-cooled in a narrow tube slightly below the melting point of −63.5 °C) to 166 °C (104 °C above the boiling point). For temperatures above the solvent's boiling point, a tube closed at the center (see Fig. 1) was used. The frequency of TMS in DMSO-d_6 (Table 5, column 3) was measured from 17 °C (mp 18 °C) to 180 °C. For CD_3OD, the frequency of TMS (Table 6, column 3) was measured from −111 °C (mp −99 °C) to 127 °C (bp 65.4 °C). Column 2 of these tables ($\Delta\delta$) is the observed ^{2}H peak separation in methanol or ethylene glycol used to determine the temperature.

Although this is not the principal purpose of this work, we also report the proton chemical shift of $CHCl_3$ in $CDCl_3$ (Table 4, column 8), DMSO-d_5 in DMSO-d_6 (Table 5, column 8) and CHD_2OD and CD_3OH in CD_3OD (Table 6), columns 8 and 9, all relative to dilute dissolved TMS in the respective solution.

3.4. Magnetic susceptibility effect

Since our determinations of the resonance frequencies of TMS and ^{3}He were made with the magnetic field locked to DMSO-d_6 or methanol-d_4 in a separate compartment (external lock), the observed frequencies depend on magnetic susceptibility, as well as inherent chemical shifts. Because identical lock substances were used, their susceptibilities cancel out when a comparison is made between TMS and ^{3}He, but the volume magnetic susceptibilities of ^{3}He and the very dilute solutions of TMS in $CDCl_3$, DMSO-d_6, and methanol-d_4 must be taken into account. Even at the highest gas density used (2.2 amagats), the concentration of helium is rather low, about 0.1 mol/L, as compared with a concentration of 12.4 mol/L for liquid chloroform at room temperature. The susceptibility of ^{3}He can thus be ignored. Likewise, the susceptibility of TMS can be neglected since it constitutes less than 0.3% of the solution.

Because we are interested in the temperature variation of the chemical shift of TMS, more than its value relative to ^{3}He, we are concerned primarily with the temperature coefficient of the volume magnetic susceptibility of the three solutions. Hoffman [19] reported that the magnetic susceptibility of $CDCl_3$ varied linearly with temperature over the range −70 to +30 °C, following the relation in Eq. (6):

$$\kappa = -0.776 + 9.5 \times 10^{-4} T, \tag{6}$$

where κ is the volume magnetic susceptibility in cgs units and T is in °C. Using the same measurement techniques under vacuum we found the susceptibility to be $-0.782 + 9.5 \times 10^{-4} T$, the difference being due to the removal of dissolved paramagnetic oxygen. The suscep-

Table 4
Observed frequency of dilute TMS in $CDCl_3$ and chemical shift of $CHCl_3$ relative to TMS

T (°C)	$\Delta\delta$ (ppm)	$^1H_{TMS}$ frequency (MHz)	Shape factor	Susceptibility	Adjusted frequency	δ_H (TMS)	δ_H ($CHCl_3$)	Deuterium reference
−70.3	2.319	400.1296712	0.0091	−0.8197	400.1310422	0.0507	7.3102	$CD_3OD = 61.42259392$
−60.0	2.241	400.1296751	0.0091	−0.8105	400.1310306	0.0465	7.3039	
−49.8	2.162	400.1296794	0.0091	−0.8013	400.1310195	0.0431	7.2981	
−39.1	2.078	400.1296836	0.0091	−0.7916	400.1310075	0.0386	7.2923	
−28.2	1.990	400.1296878	0.0090	−0.7816	400.1309950	0.0334	7.2865	
−17.5	1.903	400.1296921	0.0090	−0.7718	400.1309829	0.0286	7.2810	
−7.1	1.816	400.1296960	0.0090	−0.7622	400.1309708	0.0231	7.2758	
4.3	1.719	400.1297006	0.0089	−0.7516	400.1309577	0.0175	7.2704	
16.4	1.613	400.1297050	0.0089	−0.7403	400.1309432	0.0101	7.2649	
27.9	1.509	400.1297064	0.0089	−0.7294	400.1309263	−0.0044	7.2597	
39.7	1.400	400.1297107	0.0088	−0.7182	400.1309120	−0.0124	7.2550	
51.3	1.289	400.1297166	0.0088	−0.7070	400.1308992	−0.0167	7.2500	
65.1	1.152	400.1297231	0.0088	−0.6936	400.1308831	−0.0239	7.2445	
31.0	1.547	400.1298755	0.0170	−0.7265	400.1310882	−0.0111	7.2585	DMSO-$d_6 = 61.42254417$
46.5	1.401	400.1298892	0.0168	−0.7116	400.1310771	−0.0183	7.2518	
60.9	1.265	400.1299023	0.0166	−0.6977	400.1310669	−0.0238	7.2459	
74.3	1.137	400.1299148	0.0164	−0.6843	400.1310572	−0.0286	7.2405	
76.3	1.119	400.1299166	0.0164	−0.6824	400.1310558	−0.0292	7.2398	
88.8	0.999	400.1299281	0.0162	−0.6697	400.1310462	−0.0345	7.2351	
100.0	0.890	400.1299392	0.0161	−0.6579	400.1310377	−0.0380	7.2308	
112.1	0.773	400.1299503	0.0159	−0.6450	400.1310273	−0.0446	7.2267	
122.9	0.668	400.1299617	0.0158	−0.6331	400.1310189	−0.0476	7.2233	
134.4	0.554	400.1299746	0.0156	−0.6200	400.1310098	−0.0505	7.2181	
144.7	0.452	400.1299871	0.0155	−0.6078	400.1310021	−0.0517	7.2140	
156.1	0.339	400.1300012	0.0153	−0.5938	400.1309928	−0.0542	7.2099	
166.4	0.236	400.1300140	0.0152	−0.5807	400.1309837	−0.0578	7.2069	

Table 5
Observed frequency of dilute TMS in DMSO-d_6 and chemical shift of DMSO-d_5 relative to TMS

T (°C)	$\Delta\delta$ (ppm)	$^1H_{TMS}$ frequency (MHz)	Shape factor	Susceptibility	Adjusted frequency	δ_H (TMS)	δ_H (DMSO-d_5)	Deuterium reference
16.8	1.609	400.1299301	0.0102	−0.6158	400.1309597	0.0524	2.5046	$CD_3OD = 61.42259392$
28.5	1.504	400.1299251	0.0101	−0.6096	400.1309444	0.0421	2.5006	
39.7	1.399	400.1299222	0.0100	−0.6036	400.1309315	0.0365	2.4975	
51.2	1.289	400.1299193	0.0100	−0.5974	400.1309181	0.0306	2.4942	
62.6	1.177	400.1299163	0.0099	−0.5911	400.1309047	0.0241	2.4904	
74.8	1.133	400.1300955	0.0099	−0.5843	400.1310725	0.0103	2.4874	DMSO-$d_6 = 61.42254417$
85.4	1.031	400.1300978	0.0098	−0.5783	400.1310647	0.0068	2.4844	
96.8	0.921	400.1301002	0.0097	−0.5717	400.1310562	0.0033	2.4816	
107.6	0.817	400.1301014	0.0097	−0.5655	400.1310470	−0.0026	2.4789	
118.3	0.712	400.1301039	0.0096	−0.5592	400.1310390	−0.0051	2.4759	
128.8	0.609	400.1301054	0.0096	−0.5529	400.1310301	−0.0095	2.4734	
138.8	0.511	400.1301066	0.0095	−0.5469	400.1310213	−0.0142	2.4710	
149.2	0.408	400.1301081	0.0094	−0.5406	400.1310122	−0.0183	2.4684	
159.4	0.306	400.1301096	0.0094	−0.5344	400.1310032	−0.0221	2.4660	
169.5	0.205	400.1301108	0.0093	−0.5281	400.1309939	−0.0265	2.4633	
179.5	0.104	400.1301120	0.0093	−0.5218	400.1309846	−0.0306	2.4611	

tibility of regular chloroform in the literature is −0.740 at 20 °C [20] compared with our value of −0.763 for the evacuated $CDCl_3$ sample.

Some recent deuterium chemical shift measurements by P. Granger and M. Pioto (private communication) at the magic angle (where no susceptibility correction is required) were compared with our vertical measurements (shape factor $\alpha = 0.065$, as discussed in Appendix A) in order to calculate the solvent susceptibility from Eq. (7):

$$\kappa = \frac{\Delta\delta_{\text{vertical}} - \Delta\delta_{\text{magic}}}{(4\pi/3) - \bar{\alpha}} + \kappa_0. \tag{7}$$

Here κ_0, the known susceptibility for D_2O at 24 °C (−0.7037), is used as a standard. The values of $\Delta\delta$ represent the differences in chemical shift between the solvent

Table 6
Observed frequency of dilute TMS in CD_3OD and chemical shift of the solvent relative to TMS

T (°C)	$\Delta\delta$ (ppm)	$^1H_{TMS}$ frequency (MHz)	Shape factor	Susceptibility	Adjusted frequency	δ_H (TMS)	δ_H (CHD_2OD)	δ_H (CD_3OH)	Deuterium reference
−110.6	2.658	400.1299984	0.0189	−0.6186	400.1310305	−0.0743	3.2737	5.8765	$CD_3OD = 61.42259392$
−103.1	2.574	400.1300014	0.0189	−0.6125	400.1310234	−0.0744	3.2755	5.8200	
−91.7	2.481	400.1300020	0.0188	−0.6037	400.1310092	−0.0827	3.2782	5.7721	
−81.3	2.402	400.1300018	0.0188	−0.5959	400.1309962	−0.0904	3.2807	5.6905	
−74.3	2.349	400.1300007	0.0187	−0.5909	400.1309866	−0.0975	3.2829	5.6412	
−59.5	2.237	400.1300010	0.0187	−0.5807	400.1309700	−0.1038	3.2871	5.5366	
−49.1	2.157	400.1300009	0.0186	−0.5738	400.1309584	−0.1080	3.2891	5.4604	
−38.4	2.073	400.1300005	0.0186	−0.5670	400.1309466	−0.1121	3.2919	5.3788	
−27.3	1.983	400.1300001	0.0185	−0.5600	400.1309345	−0.1157	3.2946	5.2931	
−16.3	1.893	400.1299999	0.0185	−0.5532	400.1309230	−0.1182	3.2968	5.2062	
−5.2	1.800	400.1299996	0.0184	−0.5465	400.1309115	−0.1205	3.2990	5.1163	
6.3	1.701	400.1299994	0.0184	−0.5395	400.1308996	−0.1227	3.3014	5.0206	
17.7	1.601	400.1299990	0.0183	−0.5326	400.1308877	−0.1253	3.3035	4.9233	
30.3	1.487	400.1299987	0.0183	−0.5248	400.1308746	−0.1282	3.3055	4.8126	
45.5	1.344	400.1299984	0.0182	−0.5153	400.1308583	−0.1326	3.3083	4.6738	
60.7	1.196	400.1299982	0.0181	−0.5054	400.1308416	−0.1381	3.3107	4.5284	
75.7	1.043	400.1299980	0.0180	−0.4952	400.1308243	−0.1455	3.3131	4.3812	
4.9	1.847	400.1301510	0.0184	−0.5403	400.1310526	−0.1321			DMSO-$d_6 = 61.42254417$
17.5	1.723	400.1301587	0.0183	−0.5326	400.1310476	−0.1296			
33.5	1.568	400.1301645	0.0182	−0.5228	400.1310370	−0.1358			
50.8	1.398	400.1301730	0.0182	−0.5118	400.1310272	−0.1372			
59.5	1.312	400.1301760	0.0181	−0.5062	400.1310206	−0.1415			
74.7	1.163	400.1301829	0.0180	−0.4958	400.1310103	−0.1452			
89.9	1.014	400.1301915	0.0180	−0.4850	400.1310009	−0.1460			
101.7	0.897	400.1301981	0.0179	−0.4760	400.1309925	−0.1483			
114.4	0.773	400.1302061	0.0179	−0.4659	400.1309836	−0.1500			
126.4	0.654	400.1302140	0.0178	−0.4557	400.1309745	−0.1525			

Table 7
Measurement of susceptibility using magic angle measurements

Solvent	$^D\delta$ (magic angle) [21]	T (°C)	$^D\delta$ (vertical)	T (°C)	κ	χ_M
$CDCl_3$	7.053	27	7.202	25	−0.7318	58.73
D_2O	4.531	27	4.796	24	−0.7037	12.76
CD_3OD	3.009	27	4.000	26	−0.5277	21.43
	4.523		5.530			
DMSO-d_6	2.397	27	3.038	23	−0.6125	43.33

and D_2O, as given in Table 7. This method is more accurate than the technique described previously [19], but measurements from the two methods generally agree within their expected experimental errors.

There appear to be no data in the literature for the temperature variation of the susceptibilities of our three deuterated solvents or their undeuterated counterparts. However, density data of liquid chloroform, methanol, and dimethylsulfoxide [12] can be used to estimate the temperature coefficient of susceptibility provided we assume that the molar susceptibility is independent of temperature and that the density variation with temperature is not affected significantly by isotopic substitution. The molar susceptibility of water varies by just over 1% over its liquid range [20], and the intermolecular interactions in chloroform, DMSO, and methanol are weaker than those of water. Therefore the assumption of constant molar susceptibility appears reasonable. Likewise, the ratio of the densities of H_2O and D_2O at 10 and 100 °C differ by less than 0.3%, so the density data for ordinary solvents should be a close approximation to those for the deuterated solvents.

For chloroform, we found that over the temperature range −65 to +65 °C the density data could be approximated to a straight line. After normalization with the accepted value of the molar susceptibility, 58.9 [20], the slope of this line gives a temperature coefficient for volume susceptibility of $+9.28 \times 10^{-4}$ over this range, in very good agreement with the value cited above. However, to be able to interpolate results over wider temperature ranges for chloroform, methanol, and DMSO, we used the more complex expressions shown in Fig. 5. The volume susceptibilities (in cgs units), as computed from Eqs. (8)–(10), along with the molar susceptibilities from Table 7, are given in the fifth column of Tables 4–6.

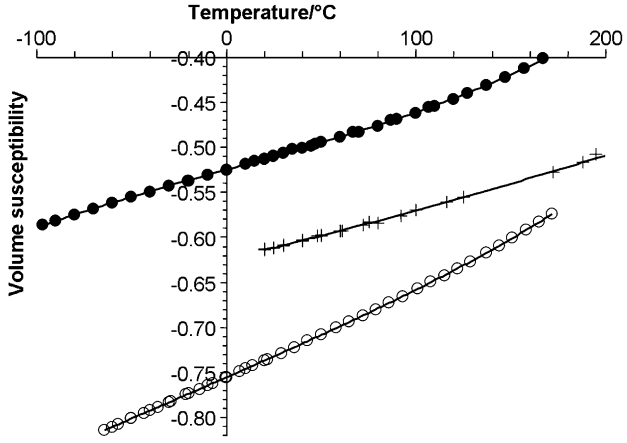

Fig. 5. Volume magnetic susceptibility of: (○) $CDCl_3$, (+) DMSO-d_6, and (●) CD_3OD determined as described in the text. For interpolation, the following expressions were determined from a least squares fit:

$$\kappa_{CDCl_3} = 1.18 \times 10^{-11} T^4 + 8.8 \times 10^{-10} T^3 + 2.57 \times 10^{-7} T^2 + 9.27 \times 10^{-4} T - 0.7556, \quad (8)$$

$$K_{\text{DMSO-}d_6} = 3.30 \times 10^{-7} T^2 + 5.13 \times 10^{-4} T - 0.6245, \quad (9)$$

$$\kappa_{CD_3OD} = 5.76 \times 10^{-10} T^3 - 4.0 \times 10^{-8} T^2 + 6.06 \times 10^{-4} T - 0.5433. \quad (10)$$

The susceptibility correction to a measured chemical shift follows Eq. (11):

$$\delta = \delta_o + \left(\frac{4\pi}{3} - \bar{\alpha}\right)\kappa, \quad (11)$$

where δ is the chemical shift, δ_o is the observed (uncorrected) chemical shift, $\bar{\alpha}$ is the mean shape factor, and κ is the volume susceptibility.

3.5. Shape factor

The shape factor for an infinite cylinder aligned with the magnetic field is zero, giving a correction for magnetic susceptibility of $(4\pi/3)\kappa = 4.189\kappa$. As indicated previously, the inner sample tube containing TMS in $CDCl_3$ had an inner diameter of 1.7 mm and a length of about 55 mm—an aspect ratio that is about 2.5 times closer to "infinite" than the typical 4.20 mm ID NMR sample tube. More precise values of the shape factor, calculated as described in Appendix A, are listed in the fourth column of Tables 4–6. As expected, these values are very small but vary with temperature as the liquid expands. Overall, they result in a correction varying from 4.170κ to 4.180κ.

3.6. Susceptibility corrections

The observed frequencies of TMS (column 3 of Tables 4–6) were adjusted to account for susceptibility according to Eq. (11), using the shape factors and susceptibility values in columns 4 and 5. Use of 4.189κ might result in an error of about 0.01 ppm in a given chemical shift value and would have a very small effect on the temperature coefficients of the chemical shifts. Note that the diamagnetic susceptibility of the three solvents causes the magnetic field in those sample tubes to be reduced relative to that in the helium sample. Hence, the measured ^1H resonance frequencies are artificially lowered and must be increased by adding the correction computed by Eq. (11). The ^1H frequencies adjusted for solvent susceptibility are given in column 6 of Tables 4–6.

3.7. ^1H chemical shift of TMS relative to ^3He

The true variation of the TMS chemical shift with temperature was determined by combining the susceptibility-adjusted data from Tables 4–6 with results interpolated from the frequency curves of ^3He (Eqs. (4) and (5)). The ^1H and ^3He data were put on a common ppm basis by computing the quantity $(\nu_T - \nu_0)/\nu_0$ for the various sets of data, with $\nu_0^H = 400.1309308$ MHz for the ^1H data (the value of the adjusted frequency for TMS in $CDCl_3$ at 25 °C, Table 5, column 6, CD_3OD lock) and $\nu_0^{He} = 304.8156473$ MHz for the ^3He data (the frequency for ^3He at 25 °C, Table 4, column 3, CD_3OD lock). The difference between the ^1H and ^3He results then provides δ, the chemical shift of TMS relative to ^3He. These values are given in column 7 of Tables 4–6, and the results are presented in Fig. 6. The trend is close to linear in all three cases, but the results can be fitted to polynomial expressions as indicated in the figure caption.

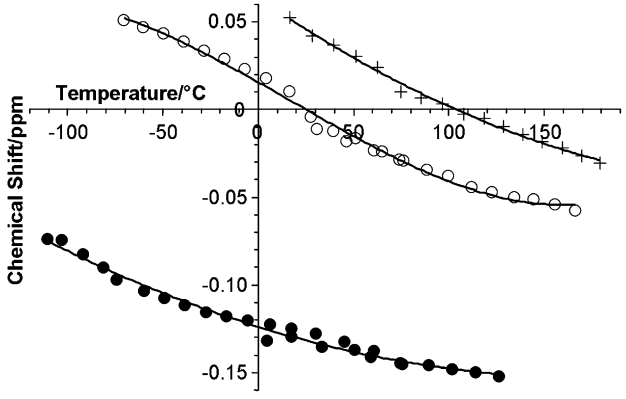

Fig. 6. ^1H chemical shift of TMS (ca. 0.1% solution) in three solutions: (○) $CDCl_3$, (+) DMSO-d_6, and (●) CD_3OD. Chemical shifts are measured relative to the ^3He resonance of ^3He gas. Least squares polynomial fits to the results are:

$$\delta(\text{TMS}/CDCl_3) = 1.040 \times 10^{-10} T^3 - 5.60 \times 10^{-7} T^2 - 6.13 \times 10^{-4} T + 0.0155, \quad (12)$$

$$\delta(\text{TMS}/\text{DMSO-}d_6) = 1.297 \times 10^{-6} T^2 - 7.49 \times 10^{-4} T + 0.0637, \quad (13)$$

$$\delta(\text{TMS}/CD_3OD) = 9.66 \times 10^{-7} T^2 - 3.35 \times 10^{-4} T - 0.1239. \quad (14)$$

4. Discussion

We believe that these results provide a reliable measure of the dependence of the ^{1}H chemical shift of TMS in $CDCl_3$, CD_3OD, and DMSO-d_6 over a wide temperature range, −111 to +180 °C. Our finding is that the temperature dependence in the three solutions is almost the same and is quite small, only about −0.0006 ppm per degree. This is considerably less than had been reported on the basis of the experiments in the 1970s and 1980s. The early work was based on the study of ^{129}Xe at natural abundance of 26% with the relatively insensitive instruments of that period and thus necessitated studies at high Xe pressure and large extrapolations, which could have introduced errors larger than the effect being sought. Our experiments benefit from high instrument sensitivity and stability and the use of 99.9% ^{3}He, which could be studied at very low pressure. Moreover, the chemical shift of ^{129}Xe is known to be affected by environmental perturbations, whereas the relatively non-polarizable ^{3}He gas should have a virtually "ideal" temperature-independent chemical shift.

The fact that the temperature dependence is small and so similar in three different solutions suggests that it should have a similar magnitude in other solutions as well. It seems reasonable that the ^{1}H methyl chemical shift in DSS, which is an IUPAC-recommended reference for aqueous solutions [21], would have a similar temperature coefficient, but this could be verified by making measurements with the deuterium locks used here and relating those data to our ^{3}He results.

A possible source of error in our results is the correction for magnetic susceptibility because of uncertainties in the volume susceptibility data and the shape factor used for the correction. It is clear from Tables 4–6 that the susceptibility correction is quite significant—large enough, in fact, to change what would appear to be a positive temperature coefficient from the observed data in column 3 to the negative coefficient arising from the corrected data. Although there are uncertainties in the susceptibility corrections arising from the assumptions described previously, we believe that they are unlikely to influence our final results by more than a few percent.

We have been careful to include detailed tables of observed data, which can be used by future experimenters along with any improved susceptibility correction data. Also, our measurements of the ^{3}He resonance frequency cover a range of −110 to +185 °C, hence can be used with new data for other solvents without having to repeat the ^{3}He study.

TMS in $CDCl_3$, the IUPAC recommended standard, is not a suitable reference at high temperature because it is quite inconvenient to use. However, our results indicate that methanol and DMSO can be used as low-temperature and high-temperature solvents, respectively, with a similar temperature dependence of the TMS chemical shift.

Acknowledgments

We thank the Margaret Thatcher Center of Interdepartmental Scientific Equipment for NMR facilities. This work was undertaken as part of an IUPAC Project [6] and was supported in part by IUPAC. The results presented here will be submitted to the project task group for inclusion in their report and eventual publication as an IUPAC Recommendation after appropriate review and public comment. Until then, these results should not be considered as having been endorsed by IUPAC. We thank other members of the IUPAC task group, especially Robin Harris and Pierre Granger, for useful discussions.

Appendix A. Calculation of the shape factor

The approximation to an infinite cylinder for the $CDCl_3$ sample is not sufficient and leads to an error of up to 0.012 ppm. We therefore approximated it to a finite cylinder. At any point along the cylindrical axis (where z is the height of the point above the center, h is the height of the cylinder, and R is the radius of the cylinder), the shape factor is given as follows (Eqs. (15) and (16)). Numerical integration of a narrow tube shows that there is little variation in shape factor across a horizontal slice unless it is close to the end, which, in our case, is sufficiently far from the receiver coil. The response profile of the probe was measured using a 1D gradient image using a calibrated gradient applied throughout acquisition. It is sufficient to approximate the response profile to a uniform region of height 16.6 mm around the center. The shape factor was averaged over this region (Eq. (17)). The depth of the liquid was measured at room temperature and calculated for other temperatures using density data for chloroform, DMSO, and methanol [12] (Eqs. (18)–(20)).

The shape factor at a point is an integral over the bounding surface of the depth (in the direction of the field) below the point being observed ($\mathbf{x}_0$) multiplied by the cosine of the angle subtended by the field to the normal to the surface (β) divided by the cube of the distance of the surface ($\mathbf{x}'$) from the observation point. It is expressed mathematically as follows Eq. (15) [22,23]:

$$\alpha(\mathbf{x}_0) = \int \cos\beta \frac{[(\mathbf{x}_0 - \mathbf{x}') \cdot \hat{\mathbf{z}}]}{|\mathbf{x}_0 - \mathbf{x}'|^3} \, \mathrm{d}s, \tag{15}$$

where $\alpha(\mathbf{x}_0)$ is the shape factor at point $\mathbf{x}_0$, β is the angle between the normal and the field at each surface element, $\hat{\mathbf{z}}$ is the unit vector along the magnetic field (z axis) and s is a surface element. The walls of the cylinder do not contribute to the shape factor because, $\cos\beta$ is zero, so one only has to integrate over the ends of the cylin-

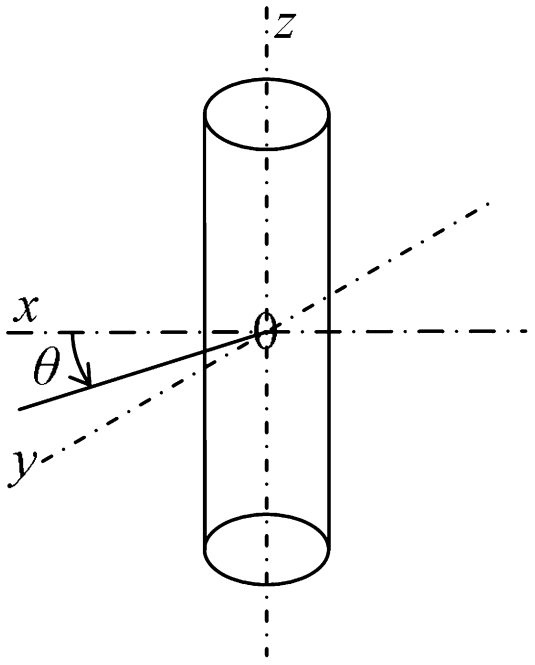

Fig. 7. Cylindrical coordinates.

der. For this, it is most convenient to use cylindrical coordinates (r,θ,h) (Fig. 7), such that $\mathrm{d}s = r\,\mathrm{d}r\,\mathrm{d}\theta$, where the origin is at the center of the cylinder (Eq. (15)). For the ends, $\cos\beta = 1$, the vertical distance from the center is $(\mathbf{x}_0 - \mathbf{x}')\cdot\hat{\mathbf{z}} = (z \pm h/2)$ the full distance from the origin is $\mathbf{x}_0 - \mathbf{x}' = \sqrt{r^2 + (z \pm h/2)^2}$. The result of Eq. (16) is then integrated over the reception region to yield the average shape factor Eq. (17).

$$
\begin{aligned}
a(0,0,z) &= \int_0^{2\pi}\int_0^{R} \frac{z-h/2}{\left[r^2+(z-h/2)^2\right]^{1.5}} \\
&\quad - \frac{z+h/2}{\left[r^2+(z+h/2)^2\right]^{1.5}} r\,\mathrm{d}r\,\mathrm{d}\theta \\
&= \int_0^{2\pi} \left[\frac{h/2-z}{\sqrt{r^2+(z-h/2)^2}} + \frac{h/2+z}{\sqrt{r^2+(z+h/2)^2}} \right]_0^{R} \mathrm{d}\theta \\
&= \int_0^{2\pi} -\frac{h/2-z}{z-h/2} + \frac{h/2+z}{z+h/2} - \frac{h/2-z}{\sqrt{R^2+(z-h/2)^2}} \\
&\quad - \frac{h/2+z}{\sqrt{R^2+(z+h/2)^2}}\,\mathrm{d}\theta \\
&= \int_0^{2\pi} 2 - \frac{h-2z}{\sqrt{4R^2+(2z-h)^2}} - \frac{h+2z}{\sqrt{4R^2+(2z+h)^2}}\,\mathrm{d}\theta \\
&= 2\pi\left(2 - \frac{h-2z}{\sqrt{4R^2+(2z-h)^2}} - \frac{h+2z}{\sqrt{4R^2+(2z+h)^2}}\right),
\end{aligned}
\tag{16}
$$

$$
\bar{\alpha} = \frac{\int_{-l}^{l} \alpha(0,0,z)\,\mathrm{d}z}{2z}. \tag{17}
$$

The average shape factor for sample $CDCl_3$ 1 was calculated to be approximately $-2.7\times10^{-6}T + 9.0\times10^{-3}$, for sample $CDCl_3$ 2 it was $-1.33\times10^{-5}T + 1.74\times10^{-2}$, for DMSO-$d_6$ it was $-5.4\times10^{-6}T + 1.03\times10^{-2}$ and for CD_3OD is was $-4.6\times10^{-6}T + 1.84\times10^{-2}$ by combining Eq. (15) (where $2l$ is the receiver coil length) with the expansion rate of chloroform and DMSO.

The volumes of $CDCl_3$, DMSO-d_6, and CD_3OD relative to their volumes at 22 °C (V_0 in Table 1) are given by Eqs. (18)–(20), which represent least squares fits to data in the AICHE DIPPR database [12].

$$
\begin{aligned}
V/V_0 &= 6.4\times10^{-11}T^4 - 7.6\times10^{-10}T^3 + 1.70\times10^{-6}T^2 \\
&\quad + 1.22\times10^{-3}T + 0.981 \text{ for } CHCl_3,
\end{aligned}
\tag{18}
$$

$$
\begin{aligned}
V/V_0 &= 2.00\times10^{-6}T^2 + 7.1\times10^{-4}T \\
&\quad + 0.983 \text{ for DMSO},
\end{aligned}
\tag{19}
$$

$$
\begin{aligned}
V/V_0 &= 1.82\times10^{-8}T^3 + 1.25\times10^{-6}T^2 + 1.04\times10^{-3}T \\
&\quad + 0.975 \text{ for } CD_3OD.
\end{aligned}
\tag{20}
$$

The volume of liquid where the liquid overflows point b (Fig. 1) is given by Eq. (21).

$$
V = \pi\left[(c-b)1.24^2 + (b-e)0.85^2\right]. \tag{21}
$$

The height of the liquid (c) where the liquid overflows point b is given by Eq. (22):

$$
c = \frac{V/\pi - (b-e)0.85^2}{1.24^2} + b, \tag{22}
$$

where the liquid does not overflow point b the volume of the liquid is given by Eq. (23).

$$
V = \pi(c-e)0.85^2. \tag{23}
$$

The height of the liquid is given by Eqs. (24)–(28)

$$
c = \frac{V}{0.85^2\pi} + e. \tag{24}
$$

For $CDCl_3$ 1:

$$
\begin{aligned}
c &= 33.3(6.3\times10^{-11}T^4 - 8\times10^{-10}T^3 + 1.69\times10^{-6}T^2 \\
&\quad + 1.21\times10^{-3}T + 0.973) + 29.
\end{aligned}
\tag{25}
$$

For $CDCl_3$ 2:

$$
\begin{aligned}
c &= 41.1(6.3\times10^{-11}T^4 - 8\times10^{-10}T^3 + 1.69\times10^{-6}T^2 \\
&\quad + 1.21\times10^{-3}T + 0.973) + 4.5.
\end{aligned}
\tag{26}
$$

For DMSO-d_6:

$$
c = 51.3(2.00\times10^{-6}T^2 + 7.1\times10^{-4}T + 0.983) + 1.1. \tag{27}
$$

For CD_3OD:

$$c = 43.8(1.82 \times 10^{-8}T^3 + 1.25 \times 10^{-6}T^2 + 1.04 \times 10^{-3}T + 0.975) + 5.6. \quad (28)$$

References

[1] R.K. Harris, E.D. Becker, S.M. Cabral de Menzes, R. Goodfellow, P. Granger, NMR nomenclature, nuclear spin properties and conventions for chemical shifts, Pure Appl. Chem. 73 (2001) 1795–1818;
R.K. Harris, E.D. Becker, J. Magn. Reson. 156 (2003) 323–326.

[2] A.K. Jameson, C.J. Jameson, Absolute temperature dependence of chemical shifts of lock solvents. Tetramethylsilane, hexafluorobenzene, and 1,4-dibromotetrafluorobenzene, J. Am. Chem. Soc. 95 (1973) 8559–8561.

[3] R.A. Meinzer, Ph.D. Thesis, University of Illinois, 1965.

[4] C.J. Jameson, A.K. Jameson, S.M. Cohen, Absolute temperature dependence of chemical shielding of some reference nuclei, J. Magn. Reson. 19 (1975) 385–392.

[5] F.G. Morin, M.S. Solum, J.D. Withers, D.M. Grant, D.K. Dalling, The temperature dependence of the magnetic susceptibility and proton and carbon-13 chemical shifts of tetramethylsilane, J. Magn. Reson. 48 (1982) 138–142.

[6] R.K. Harris, E.D. Becker, S.M. Cabral de Menzes, P. Granger, R.E. Hoffman, K. Zilm, NMR chemical shifts: updated conventions, IUPAC Project 2003-006-1-100, www.iupac.org.

[7] A.K. Jameson, C.J. Jameson, H.S. Gutowsky, Density dependence of ^{129}Xe chemical shifts in mixtures of xenon and other gases, J. Chem. Phys. 53 (1970) 2310–2321.

[8] R. Seydoux, P. Diehl, R.K. Mazitov, J. Jokisaari, Chemical-shifts in magnetic-resonance of the ^3He nucleus in liquid solvents and comparison with other noble gases, J. Magn. Reson. A 101 (1993) 78–83.

[9] E. Shabtai, A. Weitz, R.C. Haddon, R.E. Hoffman, M. Rabinovitz, A. Khong, R.J. Cross, M. Saunders, P.-C. Cheng, L.T. Scott, ^3He NMR of $He@C_{60}^{6-}$ and $He@C_{70}^{6-}$. New records for the most shielded and the most deshielded ^3He inside a fullerene, J. Am. Chem. Soc. 120 (1998) 6389–6393.

[10] J. Lounila, K. Oikarinen, P. Ingman, J. Jokisaari, Effects of thermal convection on NMR and their elimination by sample rotation, J. Magn. Reson. A 118 (1996) 50–54.

[11] N. Esturau, F. Sánchez-Ferrando, J.A. Gavin, C. Roumestand, M.-A. Delsuc, T. Parella, The use of sample rotation for minimizing convection effects in self-diffusion NMR measurements, J. Magn. Reson. 153 (2001) 48–55.

[12] Physical and Thermodynamic Properties of Pure Chemicals. American Institute of Chemical Engineers, Design Institute for Physical Properties, 1998–2004. See www.aiche.org for availability on-line and in printed form.

[13] L. Becker, R.J. Poreda, T.E. Bunch, Fullerenes: an extraterrestrial carbon carrier phase for noble gases, Proc. Natl. Acad. Sci. USA 97 (2000) 2979–2983.

[14] M.H. Miles, R.A. Hollins, B.F. Bush, J.J. Lagowski, R.E. Miles, Correlation of excess power and helium production during D_2O and H_2O electrolysis using palladium cathodes, J. Electroanal. Chem. 346 (1993) 99–117.

[15] A.L. Van Geet, Calibration of the methanol and glycol nuclear magnetic resonance thermometers with a static thermistor probe, Anal. Chem. 40 (1968) 2227–2229.

[16] A.L. Van Geet, Calibration of methanol nuclear magnetic resonance thermometer at low temperature, Anal. Chem. 42 (1970) 679–680.

[17] C. Ammann, P. Meier, A.E. Merbach, A simple multinuclear NMR thermometer, J. Magn. Reson. 46 (1982) 319–321.

[18] M.L. Kaplan, F.A. Bovey, H.N. Cheng, Simplified method of calibrating thermometric nuclear magnetic resonance standards, Anal. Chem. 47 (1975) 1703–1705.

[19] R.E. Hoffman, Variations on the chemical shift of TMS, J. Magn. Reson. 163 (2003) 325–331.

[20] D.R. Lide (Ed.), Handbook of Chemistry and Physics, CRC Press, Boca Raton, FL, 2004–2005.

[21] J.L. Markley, A. Bax, Y. Arata, C.W. Hilbers, R. Kaptein, B.D. Sykes, P.E. Wright, K. Wüthrich, Recommendations for the presentation of NMR structures of proteins and nucleic acids, Pure Appl. Chem. 70 (1998) 117–142.

[22] L. Li, Magnetic susceptibility quantification for arbitrarily shaped objects in inhomogeneous fields, Magn. Reson. Med. 46 (2001) 907–916.

[23] C.J. Durrant, M.P. Hertzberg, P.W. Kuchel, Magnetic susceptibility: further insights into macroscopic and microscopic fields and the sphere of Lorentz, Concepts Magn. Reson. A 18 (2003) 72–95.